Heterogeneous and Homogeneous EC and ECE Processes at Channel Electrodes: Analytical Wave Shape Theory

Peter D Morland and Richard G Compton*

Physical and Theoretical Chemistry Laboratory, Oxford University, South Parks Road, Oxford OX1 3QZ, United Kingdom

Received: June 11, 1999

Analytical theory is developed for EC and ECE processes, both homogeneous and heterogeneous, occurring at channel electrodes for the case where the electron transfer is electrochemically reversible. In particular the variation of the half-wave potential with solution flow rate and/or cell geometry is shown to provide a sensitive indication of electrode reaction mechanism type. Simple expressions are presented which allow the ready mechanistic interpretation of experimental data and the deduction of corresponding rate constants.

Introduction

Channel electrodes (Figure 1) have found widespread application for the resolution of electrode reaction mechanisms in which heterogeneous electron-transfer reactions are coupled with homogeneous chemical reactions.[1] There are two particular merits of conducting experimental investigations with this choice of electrode design. First, the electrode response is readily predicted, via numerical simulation, for a generality of mechanistic types so that a wide range of candidate mechanisms can be explored by the experimentalist in the context of any particular system of interest.[2,3] Second, mechanistic inferences may be sensitively made by means of a channel electrode array, with electrodes ranging in size from the millimeter to the submicrometer scale so that voltammograms measured as a function of both electrode size and solution flow rate are used to generate a form of "two-dimensional voltammetry" which provides a pair of complementary mass transport components by which to study electrode processes.[4] In both contexts it is valuable if, for relatively uncomplicated mechanistic pathways, simple analytical expressions are available to permit the interpretation of experimental data without recourse to computation.

In this paper, the analytical theory of EC and ECE processes at channel electrodes is developed for both heterogeneous and homogeneous chemical reaction in terms of the voltammetric wave shape and, in particular, the dependence of the half-wave potential on the coupled chemistry and the cell geometry. These mechanisms may be understood with reference to the following scheme:

$$\text{E step:}\quad A \pm e^- \rightarrow B \qquad \text{(i)}$$

$$\text{C step:}\quad B \rightarrow C \qquad \text{(ii)}$$

$$\text{E step:}\quad C \pm e^- \rightarrow \text{products} \qquad \text{(iii)}$$

Steps (i) and (ii) define a pure EC mechanism, while steps (i), (ii), and (iii) correspond to an ECE reaction. In effect the mechanisms differ in terms of the electroactivity of the product, C, of reaction (ii) so that if C is more readily oxidized/reduced than A the process is of the ECE type, whereas if C is electrochemically inert the process is designated EC. If step (ii) occurs in solution, the EC or ECE reactions are homogeneous in nature, whereas if the formation of C only occurs after adsorption of B on the electrode

$$B(ads) \rightarrow C(ads)$$

they are specified as heterogeneous.[5] We note that while transport limited currents have been widely used for mechanistic insight in the context of channel electrode hydrodynamic voltammetry,[1,6] only more recently has wave shape analysis been exploited[7−10] since finite element modeling has elucidated the conditions whereby the channel flow cell may be used without ohmic distortion in nonaqueous media.[11]

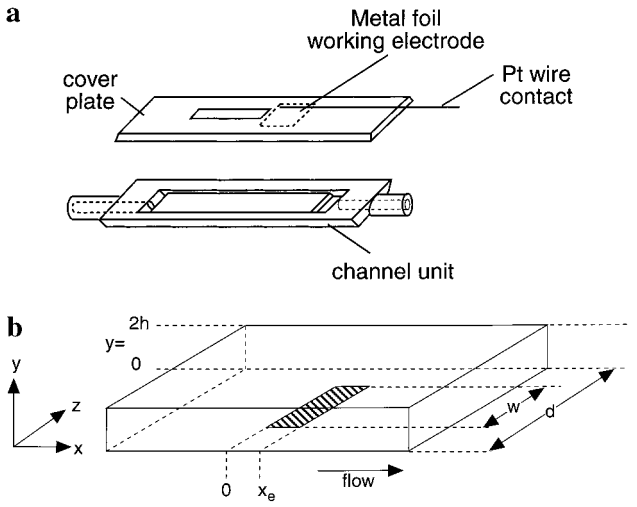

Figure 1. (a) Practical channel flow cell for mechanistic electrochemical studies. (b) Schematic diagram which defines the coordinate system adopted in the text.

Theory

We consider the EC and ECE mechanisms as defined above focusing on the specific case of a reduction and assume that the A/B redox couple is electrochemically reversible so that the Nernst Equation is applicable:

$$\frac{[A]_{y=0}}{[B]_{y=0}} = \exp(\theta) = \exp\left(\frac{F}{RT}(E - E^{\circ\prime})\right) \qquad (1)$$

10.1021/jp991922v CCC: $18.00
Published on Web 10/04/1999

where the *y*-coordinate is that normal to the electrode surface (Figure 1) and $E^{\circ\prime}$ is the formal potential of the A/B couple.

Homogeneous EC and ECE Processes. Taking first the case of the homogeneous mechanisms, the convective-diffusion equations describing the steady-state distributions of the species A, B, and C are as follows.

$$\frac{\partial[\mathrm{A}]}{\partial t} = 0 = D_{\mathrm{A}}\frac{\partial^2[\mathrm{A}]}{\partial y^2} - \upsilon_x\frac{\partial[\mathrm{A}]}{\partial x} \tag{2}$$

$$\frac{\partial[\mathrm{B}]}{\partial t} = 0 = D_{\mathrm{B}}\frac{\partial^2[\mathrm{B}]}{\partial y^2} - \upsilon_x\frac{\partial[\mathrm{B}]}{\partial x} - k_{(\mathrm{ii})}[\mathrm{B}] \tag{3}$$

$$\frac{\partial[\mathrm{C}]}{\partial t} = 0 = D_{\mathrm{C}}\frac{\partial^2[\mathrm{C}]}{\partial y^2} - \upsilon_x\frac{\partial[\mathrm{C}]}{\partial x} + k_{(\mathrm{ii})}[\mathrm{B}] \tag{4}$$

where D_{X} is the diffusion coefficient of species X (= A, B or C), $k_{(\mathrm{ii})}$ is the rate constant corresponding to reaction (ii), and the Cartesian coordinate *x* is that in the direction of flow (Figure 1). υ_x is the solution velocity in the *x*-direction; the components in the *y*- and *z*-directions are zero. Given laminar flow conditions and that a sufficiently long lead-in length exists upstream of the electrodes so as to allow the full development of Poiseuille flow, then υ_x is parabolic:

$$\upsilon_x = \upsilon_{\mathrm{o}}\left(1 - \frac{(h-y)^2}{h^2}\right) \tag{5}$$

where *h* is the half-height of the cell and υ_{o} is the solution velocity at the center of the channel.[12] Equations 2−4 assume that axial diffusion effects may be neglected; this is valid provided the electrodes considered are not of microelectrode dimensions.[13]

The relevant boundary conditions in addition to eq 1 are as follows.

EC mechanism

$$\text{all } y, x < 0: \quad [\mathrm{A}] = [\mathrm{A}]_{\mathrm{bulk}}, \quad [\mathrm{B}] = 0, \quad [\mathrm{C}] = 0 \tag{6}$$

$$y = 0,\ 0 < x < x_{\mathrm{e}}: \quad D_{\mathrm{A}}\frac{\partial[\mathrm{A}]}{\partial y} = -D_{\mathrm{B}}\frac{\partial[\mathrm{B}]}{\partial y} \tag{7}$$

$$y = 0,\ 0 < x < x_{\mathrm{e}}: \quad D_{\mathrm{C}}\frac{\partial[\mathrm{C}]}{\partial y} = 0 \tag{8}$$

$$y = 2h, \text{ all } x: \quad D_{\mathrm{A}}\frac{\partial[\mathrm{A}]}{\partial y} = D_{\mathrm{B}}\frac{\partial[\mathrm{B}]}{\partial y} = D_{\mathrm{C}}\frac{\partial[\mathrm{C}]}{\partial y} = 0 \tag{9}$$

ECE mechanism

$$\text{all } y, x < 0: \quad [\mathrm{A}] = [\mathrm{A}]_{\mathrm{bulk}}, \quad [\mathrm{B}] = 0, \quad [\mathrm{C}] = 0 \tag{10}$$

$$y = 0,\ 0 < x < x_{\mathrm{e}}: \quad D_{\mathrm{A}}\frac{\partial[\mathrm{A}]}{\partial y} = -D_{\mathrm{B}}\frac{\partial[\mathrm{B}]}{\partial y} \tag{11}$$

$$y = 0,\ 0 < x < x_{\mathrm{e}}: \quad [\mathrm{C}] = 0 \tag{12}$$

$$y = 2h, \text{ all } x: \quad D_{\mathrm{A}}\frac{\partial[\mathrm{A}]}{\partial y} = D_{\mathrm{B}}\frac{\partial[\mathrm{B}]}{\partial y} = D_{\mathrm{C}}\frac{\partial[\mathrm{C}]}{\partial y} = 0 \tag{13}$$

where x_{e} is the electrode length.

To develop the analytical solution of eqs 2−4, we introduce the normalized variables χ, ξ, and *K* given[1] by

$$\chi = x/x_{\mathrm{e}} \tag{14}$$

$$\xi = (2\upsilon_{\mathrm{o}}/hDx_{\mathrm{e}})^{1/3}y \tag{15}$$

$$K = k_{(\mathrm{ii})}(h^2x_{\mathrm{e}}{}^2/4\upsilon_{\mathrm{o}}{}^2D)^{1/3} \tag{16}$$

where 2*h* is the channel depth and we have assumed that $D = D_{\mathrm{A}} = D_{\mathrm{B}} = D_{\mathrm{C}}$. Next, we note that practical channel flow cells are usually designed to operate under conditions where the time to diffuse across the depth of the cell is long compared to that required to convect along the electrode length (x_{e})[1] so that

$$\{(2h)^2/D\} \gg (x_{\mathrm{e}}/\upsilon_0) \tag{17}$$

As a result, concentration changes induced electrolytically are confined to locations in the *y*-direction which are close to the electrode surface. The velocity profile in the *x*-direction, υ_x, may be approximated near $y = 0$ with

$$\begin{aligned}\upsilon_x &= \upsilon_{\mathrm{o}}\left(1 - \frac{(h-y)^2}{h^2}\right)\\ &= \upsilon_{\mathrm{o}}\left(1 - \frac{h-y}{h}\right)\left(1 + \frac{h-y}{h}\right)\\ &\approx \frac{2\upsilon_{\mathrm{o}}y}{h} \quad \text{for} \quad y \approx 0\end{aligned} \tag{18}$$

This linearization of the parabolic velocity profile near $y = 0$ is the Lévêque approximation.[14]

The mass transport equations then simplify as follows.

$$0 = \frac{\partial^2[\mathrm{A}]}{\partial\xi^2} - \xi\frac{\partial[\mathrm{A}]}{\partial\chi} \tag{19}$$

$$0 = \frac{\partial^2[\mathrm{B}]}{\partial\xi^2} - \xi\frac{\partial[\mathrm{B}]}{\partial\chi} - K[\mathrm{B}] \tag{20}$$

$$0 = \frac{\partial^2[\mathrm{C}]}{\partial\xi^2} - \xi\frac{\partial[\mathrm{C}]}{\partial\chi} + K[\mathrm{B}] \tag{21}$$

We focus first on the EC mechanism and apply the Laplace transform technique[15] defining the Laplace transform, with respect to χ, of the concentration of A as follows where *s* is the transformed variable of χ:

$$L[\mathrm{A}] = \int_0^\infty \exp(-s\chi)[\mathrm{A}]\,\mathrm{d}\chi \tag{22}$$

Application of the Laplace transform[15] to eqs 19−21 and the use of the pertinent boundary conditions gives

$$\frac{L[\mathrm{A}]}{[\mathrm{A}]_{\mathrm{bulk}}} = \left(\frac{1}{s} - \frac{Ai(s^{1/3}\xi)}{s\,Ai(0)} + \frac{Ai'(0)\exp(\theta)\,Ai(s^{-2/3}K)\,Ai(s^{1/3}\xi)}{s(\exp(\theta)\,Ai'(0)\,Ai(0)\,Ai(s^{-2/3}K) + Ai(0)^2\,Ai(s^{-2/3}K))}\right) \tag{23}$$

where $Ai(x)$ denotes the Airy function[16,17]

$$Ai(x) = \frac{1}{3^{2/3}\pi}\sum_{0}^{\infty}\frac{\Gamma\left(\frac{1}{3}n+\frac{1}{3}\right)}{n!}\sin\left[\frac{2}{3}(n+1)\pi\right](3^{1/3}x)^n \quad (24)$$

which is the solution to the differential equation

$$\frac{d^2Ai(x)}{dx^2} = x\,Ai(x) \quad (25)$$

$Ai'(x)$ denotes the first derivative of $Ai(x)$.

To deduce the current (I)−voltage behavior we need to evaluate

$$I = DFw\int_0^{x_e}\left(\frac{\partial[A]}{\partial y}\right)_{y=0} dx \quad (26)$$

or

$$I = Fw\left(\frac{2v_o x_e^2 D^2}{h}\right)^{1/3}\int_0^1\left(\frac{\partial[A]}{\partial\xi}\right)_{\xi=0} d\chi \quad (27)$$

where w is the electrode width and F is the Faraday constant. Performing the integration in the transformed space[15] and applying the inverse Laplace tranform operation (L^{-1}), we find the following expression for the current.

$$I = Fw\left(\frac{2v_o x_e^2 D^2}{h}\right)^{1/3}\left[L^{-1}\left(\frac{1}{s}\frac{\partial L[A]}{\partial\xi}\right)_{\xi=0}\right]_{\chi=1} \quad (28)$$

From eq 23 it may be deduced that

$$\left(\frac{1}{s}\frac{\partial[A]}{\partial\xi}\right)_{\xi=0} = -\frac{[A]_{bulk}}{s^{5/3}}\frac{Ai'(0)}{Ai(0)}\frac{1}{1+\exp(\theta)\frac{Ai(s^{-2/3}K)\,Ai'(0)}{Ai'(s^{-2/3}K)\,Ai(0)}} \quad (29)$$

Equations 28 and 29 permit the deduction of the current−voltage ($I-\theta$) wave shape for any value of K provided the inverse Laplace transformation implied in eqs 28 and 29 can be carried out. In practice we seek approximations for small and large K. For small K we note that

$$Ai(s^{-2/3}K) = \sum_{0}^{\infty}a_n s^{-2n/3}K^n \quad (30)$$

where the coefficients a_n may be inferred from eq 24. This together with the standard inverse Laplace transform result

$$L^{-1}\Gamma(v+1)p^{-v-1} = \chi^v \quad (v > -1) \quad (31)$$

permits the deduction of the following low K approximation

$$\frac{I}{Fw\left(\frac{2v_o x_e^2 D^2}{h}\right)^{1/3}[A]_{bulk}} = -\sum_{0}^{\infty}\frac{f(n,\theta)K^n}{\Gamma\left(\frac{2n+5}{3}\right)} \quad (32)$$

where

$$f(0,\theta) = \frac{Ai'(0)}{Ai(0)(1+\exp(\theta))} \quad (33)$$

and

$$f(n,\theta) = \frac{1}{Ai(0)(1+\exp(\theta))}\left[(n+1)a_{n+1} - \sum_{i=1}^{i=n}f(n-1,\theta)\left(\frac{Ai(0)}{Ai'(0)}(i+1)a_{i+1} + \exp(\theta)a_i\right)\right] \quad (34)$$

Note when $(-\theta)\rightarrow\infty$ corresponding to the transport-limited current, I_{lim}, that

$$\frac{I}{Fw\left(\frac{2v_o x_e^2 D^2}{h}\right)^{1/3}[A]_{bulk}} \rightarrow -\frac{Ai'(0)}{Ai(0)}\frac{1}{\Gamma(5/3)} \quad (35)$$

which is independent of K and simply states the Levich equation expected for a one-electron process.[1]

Corresponding low K expressions can be deduced for at point χ on the electrode surface ($0 < \chi < 1$), for the current density, i

$$\frac{i}{Fw\left(\frac{2v_o x_e^2 D^2}{h}\right)^{1/3}[A]_{bulk}} = -\sum_{j=0}^{\infty}\frac{f(j,\theta)K^j\chi^{(2j-1)/3}}{\Gamma\left(\frac{2j+2}{3}\right)} \quad (36)$$

and for the local concentration of A at different points over the electrode surface

$$\frac{[A]_{\chi,\xi=0}}{[A]_{bulk}} = \sum_{n=0}^{\infty}\frac{g(n)(K\chi^{2/3})^n}{\Gamma\left(\frac{2n+3}{3}\right)} \quad (37)$$

where

$$g(0) = \frac{\exp(\theta)}{\exp(\theta)+1} \quad (38)$$

and

$$g(n) = [a_n Ai'(0)\exp(\theta) - \sum_{j=1}^{i=n}g(n-i)(Ai'(0)\,a_i\exp(\theta) + (i+1)\,Ai(0)\,a_{i+1})]/[Ai'(0)\,Ai(0)\exp(\theta) + Ai'(0)\,Ai(0)] \quad (39)$$

To develop a high K approximation, we return to eq 20 and recognize that if B is sufficiently short-lived then it is only distributed within a thin reaction layer of a thickness which is significantly smaller than the diffusion layer of the channel electrode so that

$$0 \approx \frac{\partial^2[B]}{\partial\xi^2} - K[B] \quad (40)$$

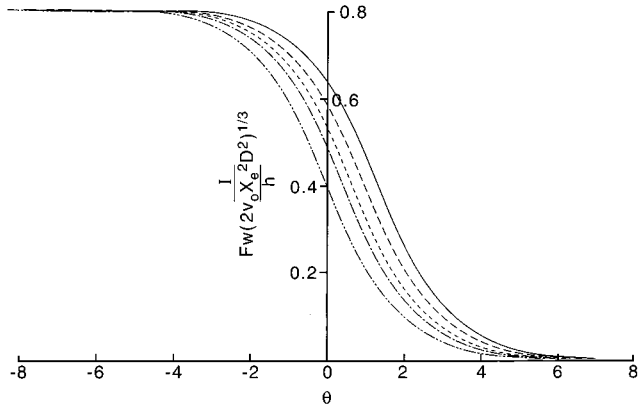

Figure 2. Current−voltage ($I-\theta$) curves calculated for the homogeneous EC mechanism using the low K approximation of eq 35 for the following values of K: 0, 1.0, 2.0, 4.0, and 8.0.

Solution of this equation, application of the appropriate boundary conditions, and Laplace transformation give the approximate result that

$$L[\mathrm{B}] = \exp(-\theta - K^{1/2}\xi)\, L[\mathrm{A}]_{\xi=0} \tag{41}$$

Solution of eq 19 and using eq 41 to provide a boundary condition via eq 7 give the following

$$\frac{L[\mathrm{A}]_{\xi=0}}{[\mathrm{A}]_{\mathrm{bulk}}} = \left(\frac{Ai'(0)}{s^{2/3}\,Ai(0)}\right)\frac{1}{\left[\dfrac{s^{1/3}Ai'(0)}{Ai(0)} - K^{1/2}\exp(-\theta)\right]} \tag{42}$$

Expanding as a power series in $s^{1/3}$ together with eqs 7, 27, and 41 then gives the result that

$$\frac{I}{Fw\left(\dfrac{2v_o\chi_e^2D^2}{h}\right)^{1/3}[\mathrm{A}]_{\mathrm{bulk}}} \approx \sum_{n=0}^{4}\left(\frac{\exp(\theta)}{K^{1/2}}\right)^n\left(\frac{Ai'(0)}{Ai(0)}\right)^{n+1}\frac{1}{\Gamma\left(\dfrac{5-n}{3}\right)} \tag{43}$$

where the summation is limited by the number of terms that are Laplace-invertable via eq 31. Equations 32 and 43 respectively give low K and high K approximations to the current−voltage wave shape for a homogeneous EC process. In practice the high K equation is only useful for currents such that $I/I_{\mathrm{lim}} > 0.75$ on account of the finite number of terms in the series.

Figure 2 shows voltammograms calculated using the power series given in eq 32 for values of K between 0 and 8. For larger values of K the series did not converge. For a value of $K = 1$ only 10 terms in eq 35 were required to converge the current to within 1%; for $K = 8$, 50 terms were required. The current−voltage curves shown in Figure 2 all have the shape expected for an electrochemically reversible process,

$$I = \frac{I_{\mathrm{lim}}}{1 + \exp(\theta)} \tag{44}$$

but the half-wave potential, $E_{1/2}$, is shifted progressively toward voltages more positive than $E^{\circ\prime}$ as K increases from zero to larger values. The calculated voltammograms permit the inference of the dependence of $E_{1/2}$ on K; this is shown in Figure 3, which displays the shift in the half-wave potential from the formal potential in terms of the dimensionless parameter, $\theta_{1/2}$, defined as follows.

$$\theta_{1/2} = \left(\frac{F}{RT}\right)(E_{1/2} - E^{\circ\prime}) \tag{44}$$

For $K < 3.4$ the curve shown can be described by the approximate equation

$$\theta_{1/2} = 0.0064(\ln K)^3 + 0.795(\ln K)^2 + 0.3048(\ln K) + 0.4124 \tag{45}$$

to within 2%. For $K > 5.0$ the following expression

$$\theta_{1/2} = 0.26039 + 0.5 \ln K \tag{46}$$

was found to be valid. The result that the shift in half-wave potential in the high K limit is solely a function of $K^{1/2}$ is implicit in eq 42.

The local response at different points on the electrode surface to progressively increasing values of K can be probed by means

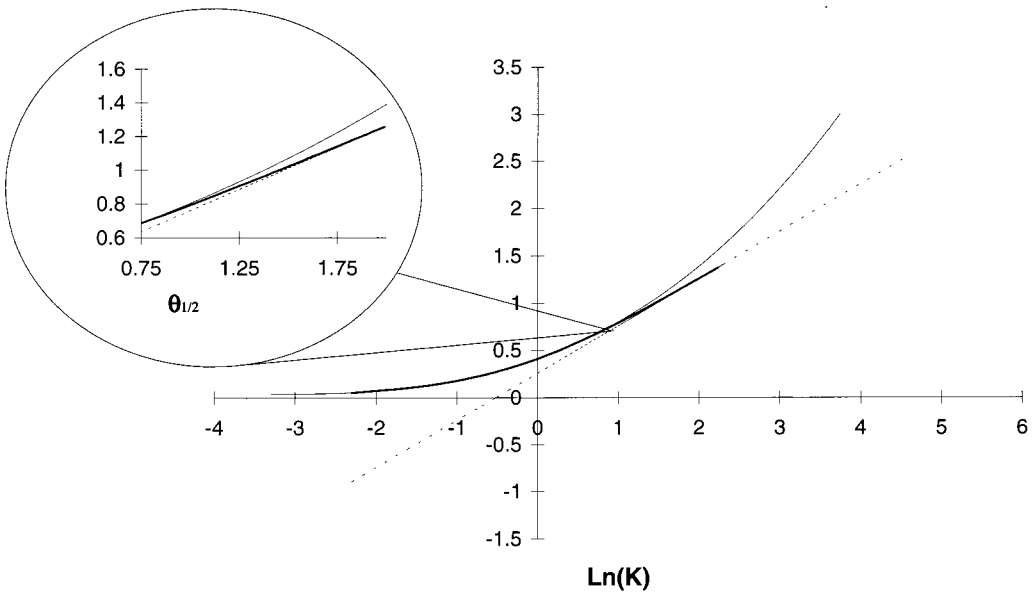

Figure 3. Variation of $\theta_{1/2}$ with ln K (bold line) as deduced from eq 43. In addition, the low K (eq 45) and high K (eq 46) approximations are shown.

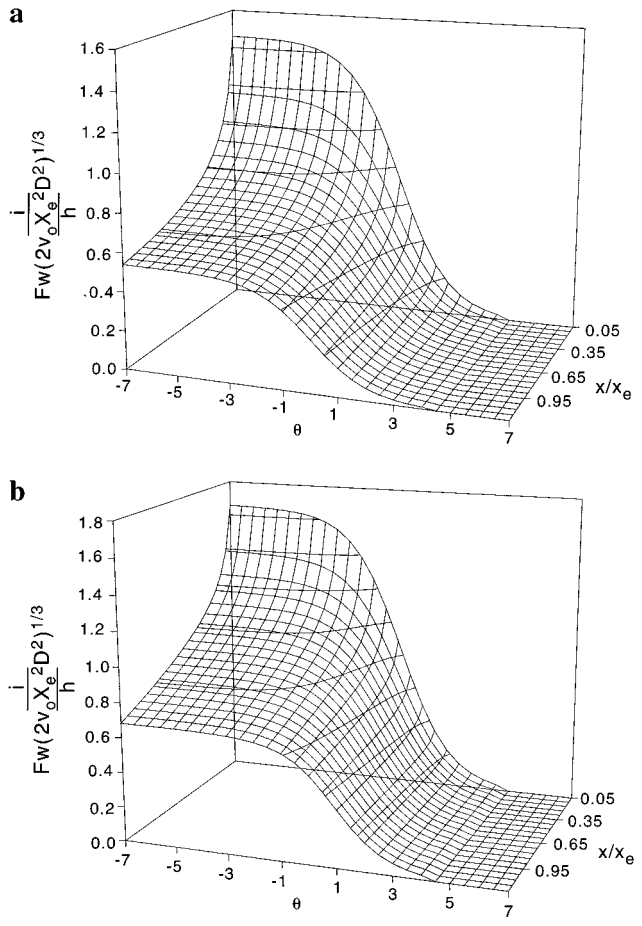

Figure 4. Current density shown as a function of θ and χ for (a) $K = 0.0$ and (b) $K = 1.0$.

of eqs 36 and 37. Figure 4 shows the current density as a function of θ and χ for $K = 0$ and 1. The high currents at the upstream edge of the electrode reflect the supply of fresh material arriving, and the steady decrease in the current density in the downstream direction is due to the consumption of A and the growth of the diffusion layer across which new electroactive material must be transported. However, plots of the difference in current density, again as a function of θ and χ, seen for a particular value of K compared to that for $K = 0$ gives useful insight. Figure 5 shows such plots for values of K of 0.2, 0.6, 1.0, and 1.4. It can be seen that for low values of K the increase in current density resulting from the anodic shift of the reductive voltammetric wave occurs predominantly downstream owing to the sluggish kinetics by which B decomposes. This species appears essentially stable in the upstream part of the electrode; only after it has travelled a significant distance downstream has the decomposition of B become significant enough to exert an appreciable effect on the voltammetry. Since the surface concentrations of A and B are linked via eq 1, the loss of B leads to enhanced electrolytic removal of A and hence an increased current density. Comparison of different plots in Figure 5 however show that as K increases this effect propagates upstream. Moreover, for values of K in excess of ca. 1.0 this effect of increased electrolysis of A in the upstream part of the electrode leads to locally decreased current densities on the downstream portion of the electrode. These inferences are confirmed by eq 37, which predicts the variation of the concentration of A over the electrode surface (χ) as a function of θ; typical results are shown in Figure 6.

We next turn to the homogeneous ECE mechanism. Laplace transformation of eqs 19−21 and application of the boundary conditions 10−13 yield the following results.

$$\frac{L[\mathrm{A}]}{[\mathrm{A}]_{\mathrm{bulk}}} = \frac{1}{s}\left(1 - \frac{Ai(s^{1/3}\xi)}{Ai(0)} + \frac{Ai(s^{1/3}\xi)}{Ai(0) + \dfrac{Ai(0)^2\, Ai'(s^{-2/3}K)}{\exp(\theta)\, Ai'(0)\, Ai(s^{-2/3}K)}}\right) \quad (47)$$

and

$$\frac{L[\mathrm{C}]}{[\mathrm{A}]_{\mathrm{bulk}}} = \frac{1}{s}\left([Ai(s^{-2/3}K)\, Ai(s^{1/3}\xi) - Ai(0)\, Ai(s^{-2/3}K + s^{1/3}\xi)]/\left[\exp(\theta)\, Ai(0)\, Ai(s^{-2/3}K) + \frac{Ai(0)^2\, Ai'(s^{-2/3}K)}{Ai'(0)}\right]\right) \quad (48)$$

We note first that eq 48 predicts that there is no C present at the electrode surface as required by the boundary conditions and second that as $K \rightarrow 0$ the concentration profile of A assumes that for an EC process as derived above.

The current−voltage behavior is given by

$$I = Fw\left(\frac{2v_o x_e^{\,2} D^2}{h}\right)^{1/3} [\mathrm{A}]_{\mathrm{bulk}}\left[L^{-1}\left(\frac{1}{s}\frac{\partial(L[\mathrm{A}] + [\mathrm{C}])}{\partial\xi}\right)_{\xi=0}\right]_{\chi=1} \quad (49)$$

From eqs 47−49 it can be seen that

$$\frac{1}{s}\frac{\partial(L[\mathrm{A}] + [\mathrm{C}])}{\partial\xi}_{\xi=0} = \frac{[\mathrm{A}]_{\mathrm{bulk}}}{s^{5/3}}([Ai'(0)^2\, Ai(s^{-2/3}K) - 2Ai(0)\, Ai'(0)\, Ai'(s^{-2/3}K)]/[\exp(\theta)\, Ai(0)\, Ai'(0)\, Ai(s^{-2/3}K) + Ai(0)^2\, Ai'(s^{-2/3}K)]) \quad (50)$$

On inversion we find the following low K approximation.

$$\frac{I}{Fw\left(\dfrac{2v_o x_e^{\,2} D^2}{h}\right)^{1/3} [\mathrm{A}]_{\mathrm{bulk}}} = -\sum_0^{\infty} \frac{d(n,\theta)K^n}{\Gamma\left(\dfrac{2n+5}{3}\right)} \quad (51)$$

where

$$d(0,\theta) = \frac{-Ai'(0)}{Ai(0)(1 + \exp(\theta))} \quad (52)$$

and

$$d(n,\theta) = \frac{1}{Ai(0)^2\, Ai'(0)(1 + \exp(\theta))} \times [Ai'(0)^2 a_n - 2(n+1)Ai(0)\, Ai'(0)a_{n+1} - \sum_{j=1}^{j=n} d(n-j,\theta)(Ai(0)\,((j+1)Ai(0)a_{j+1} + \exp(\theta)\, Ai'(0)a_j)] \quad (53)$$

It can be seen from eq 51 that as $K \rightarrow \infty$ the limiting current for the ECE mechanism tends, as expected, to twice that for an EC mechanism.

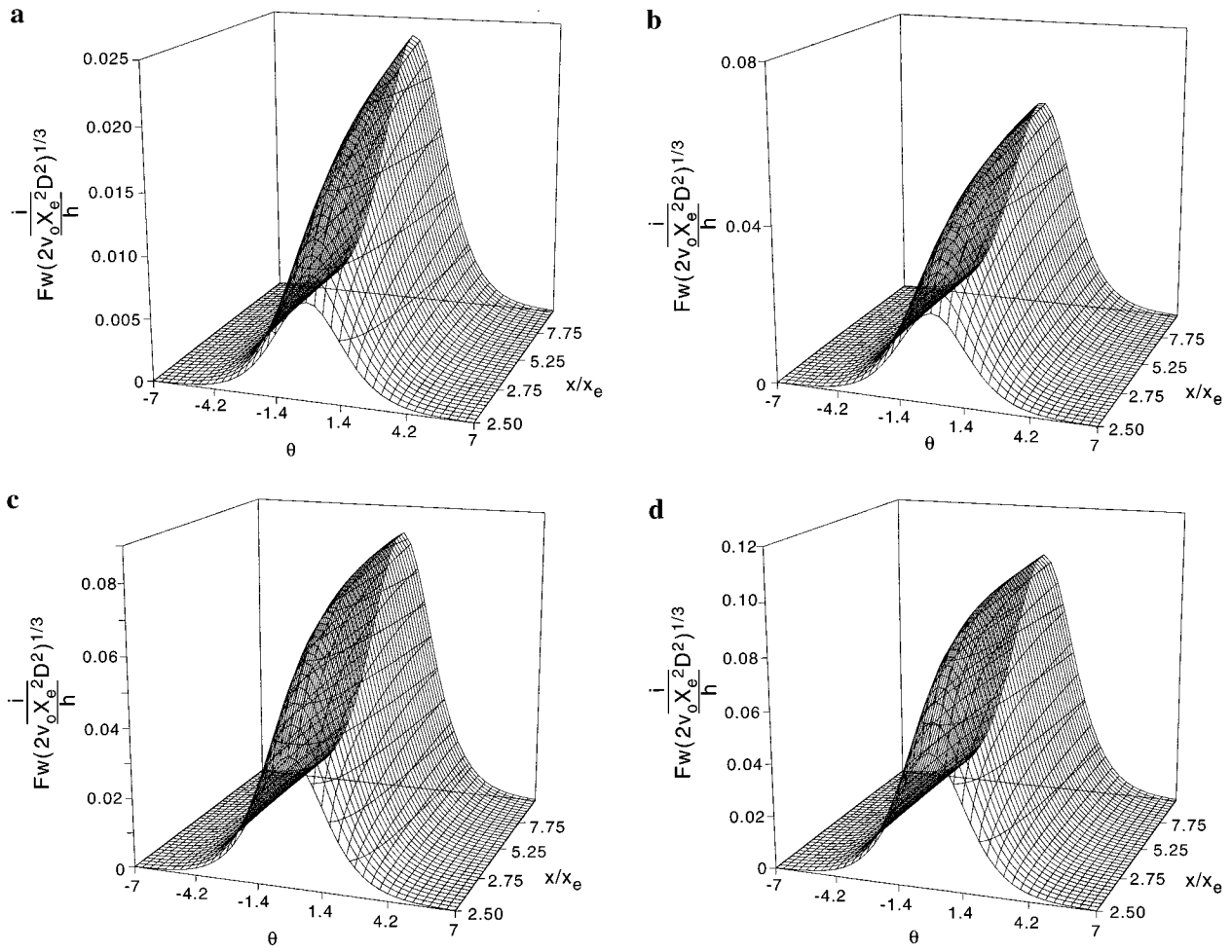

Figure 5. Difference plots showing the current density for K equal to (a) 0.2, (b) 0.6, (c) 1.0, and (d) 1.4 compared to that for K of 0 as a function of θ and χ.

Corresponding low K expressions can be deduced for the current density at any point on the electrode surface

$$\frac{i}{Fw\left(\frac{2v_o x_e{}^2 D^2}{h}\right)^{1/3}} = -[\mathrm{A}]_{\mathrm{bulk}} \sum_{j=0}^{\infty} \frac{d(j,\theta) K^j \chi^{(2j-1)/3}}{\Gamma\left(\frac{2j+2}{3}\right)} \quad (54)$$

To investigate a high K approximation, we consider eqs 20 and 21 and again note that if B is sufficiently short-lived it is only distributed within a thin reaction layer such that the convective transport of B may be neglected and eq 40 can be used in place of eq 20. Likewise instead of eq 21 we have

$$0 \approx \frac{\partial^2[\mathrm{B}]}{\partial \xi^2} + K[\mathrm{C}] \quad (55)$$

Solving eqs 19, 40, and 55 under the boundary conditions 10−13 reveals the following

$$\frac{\partial L[\mathrm{C}]}{\partial \xi} = [\mathrm{A}]_{\mathrm{bulk}} \left(\frac{Ai'(0)}{s^{2/3} Ai(0)} \frac{1}{\left(\frac{1}{s^{2/3}} \frac{\exp(\theta)}{K^{1/2}} \frac{Ai'(0)}{Ai(0)} - 1 \right)} \right) \quad (56)$$

from which a high K approximation for the current−voltage behavior can be obtained:

$$\frac{\mathrm{I}}{Fw[\mathrm{A}]_{\mathrm{bulk}} \left(\frac{2v_o x_e{}^2 D^2}{h}\right)^{1/3}} \approx \sum_{n=0}^{4} \left(\frac{\exp(\theta)}{K^{1/2}}\right)^n \left(\frac{Ai'(0)}{Ai(0)}\right)^{n+1} \frac{2}{\Gamma\left(\frac{5-n}{3}\right)} \quad (57)$$

which differs from eq 43, as expected, simply by a factor of 2.

Figure 7 shows voltammograms calculated using the power series given in eq 51 for values of K between 0 and 8.0. Again, for a value of $K = 1$, 10 terms were required to converge the current to within 1%; for $K = 8$, 50 terms were needed. As for the homogeneous EC process all the curves in Figure 7 have the shape defined by eq 44 and expected for an electrochemically reversible process. The shift in half-wave potential was found to be unchanged from that seen for the EC case; eqs 45 and 46 quantify the behavior. Finally, the curves shown in Figure 7 also allow the deduction of the effective number of electrons transferred during an ECE processes as a function of K; the data obtained was in excellent agreement with the expressions derived elsewhere for this relationship.[18]

Heterogeneous EC and ECE Processes. Considering next the case of the heterogeneous mechanisms the (dimensionless)

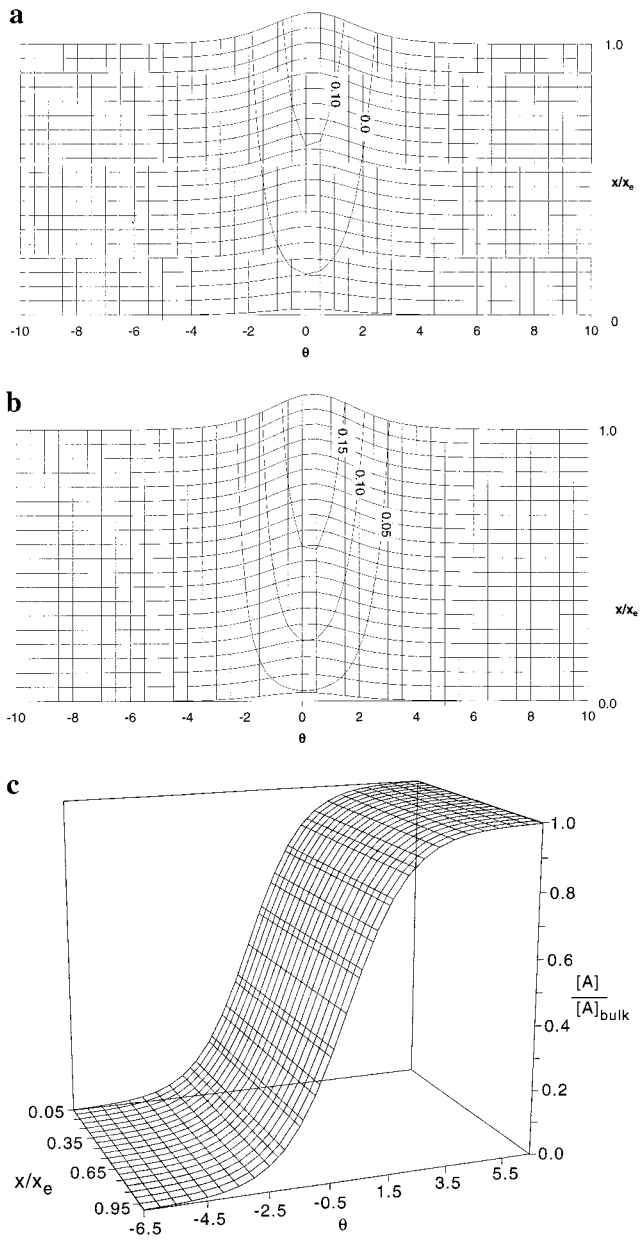

Figure 6. Change from $K = 0$ to (a) $K = 1$ and (b) $K = 2$ in the concentration of A over the electrode surface (χ) as a function of electrode potential (θ). Also shown for reference is (c) the concentration profile of A for the case where $K = 0$.

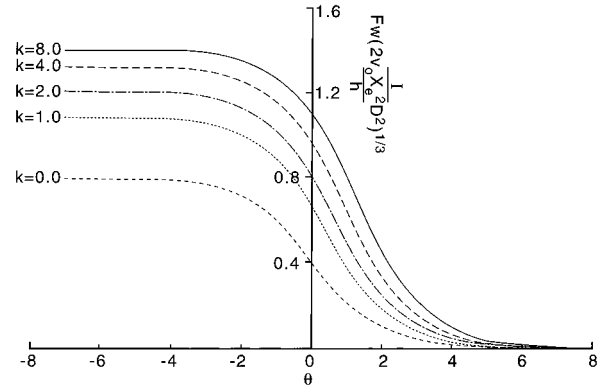

Figure 7. Current−voltage ($I-\theta$) curves calculated for the homogeneous ECE mechanism using the low K approximation of eq 51 for the following values of K: 0.0, 1.0, 2.0, 4.0, and 8.0.

convective-diffusion equations describing the steady-state distributions of A, B and C are as follows.

$$\frac{\partial[\mathrm{A}]}{\partial t} = 0 = D_{\mathrm{A}}\frac{\partial^2[\mathrm{A}]}{\partial y^2} - \upsilon_x\frac{\partial[\mathrm{A}]}{\partial x} \tag{58}$$

$$\frac{\partial[\mathrm{B}]}{\partial t} = 0 = D_{\mathrm{B}}\frac{\partial^2[\mathrm{B}]}{\partial y^2} - \upsilon_x\frac{\partial[\mathrm{B}]}{\partial x} \tag{59}$$

$$\frac{\partial[\mathrm{C}]}{\partial t} = 0 = D_{\mathrm{C}}\frac{\partial^2[\mathrm{C}]}{\partial y^2} - \upsilon_x\frac{\partial[\mathrm{C}]}{\partial x} \tag{60}$$

The boundary conditions for both mechanisms are the same as for the homogeneous cases, with the exception of eqs 7 and 11 which are replaced by

$y = 0,\ 0 < x < x_{\mathrm{e}}$:

$$D_{\mathrm{A}}\frac{\partial[\mathrm{A}]}{\partial\xi} = -D_{\mathrm{B}}\frac{\partial[\mathrm{B}]}{\partial\xi} + K_{\mathrm{het}}[\mathrm{B}]_{\xi=0} \tag{61}$$

where

$$K_{\mathrm{het}} = k_{\mathrm{het}}(hDx_{\mathrm{e}}/2\upsilon_{\mathrm{o}})^{1/3} \tag{62}$$

Application of the Laplace transform to eqs 58 and 59 together with the above boundary condition shows that

$$\frac{L[\mathrm{A}]}{[\mathrm{A}]_{\mathrm{bulk}}} = \frac{1}{s}\left(1 - \frac{Ai(s^{1/3}\xi)}{Ai(0)} + \frac{\exp(\theta)}{\exp(\theta)+1}\frac{Ai(s^{1/3}\xi)}{Ai(0)}\frac{1}{1 - \dfrac{1}{\exp(\theta)+1}\dfrac{Ai(0)}{Ai'(0)}\dfrac{K_{\mathrm{het}}}{s^{1/3}}}\right) \tag{63}$$

It follows that for a heterogeneous EC process the current−voltage behavior is given by the following low K_{het} approximation

$$\frac{I}{Fw\left(\dfrac{2\upsilon_{\mathrm{o}}x_{\mathrm{e}}{}^2D^2}{h}\right)^{1/3}[\mathrm{A}]_{\mathrm{bulk}}} = \frac{-Ai'(0)}{Ai(0)(\exp(\theta)+1)\Gamma(5/3)} + \frac{\exp(\theta)}{\exp(\theta)+1}\sum_0^\infty\left(\frac{Ai(0)}{Ai'(0)}\right)^n\left(\frac{K_{\mathrm{het}}}{(\exp(\theta)+1)}\right)^{n+1}\frac{1}{\Gamma\left(\dfrac{n+6}{3}\right)} \tag{64}$$

which in the limit $\theta \rightarrow -\infty$ collapses to the expected one electron limiting Levich current (eq 35).

Similarly, a low K_{het} expression can be derived for the local current density, i

$$\frac{i}{Fw\left(\dfrac{2\upsilon_{\mathrm{o}}x_{\mathrm{e}}{}^2D^2}{h}\right)^{1/3}[\mathrm{A}]_{\mathrm{bulk}}} = \frac{-Ai'(0)\chi^{-1/3}}{Ai(0)(\exp(\theta)+1)\Gamma(2/3)} + \frac{\exp(\theta)}{\exp(\theta)+1}\sum_0^\infty\left(\frac{Ai(0)}{Ai'(0)}\right)^n\left(\frac{K_{\mathrm{het}}}{(\exp(\theta)+1)}\right)^{n+1}\frac{\chi^{n/3}}{\Gamma\left(\dfrac{n+3}{3}\right)} \tag{65}$$

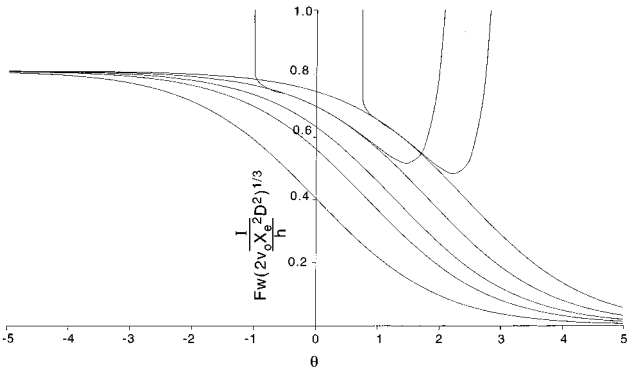

Figure 8. Current−voltage ($I-\theta$) curves calculated for the heterogeneous EC mechanism, as described in the text for the following values of K: 0.0, 1.0, 2.0, 4.0, and 8.0.

and the concentration distribution over the electrode surface

$$\frac{[A]_{\chi,\xi=0}}{[A]_{bulk}} = \frac{\exp(\theta)}{\exp(\theta)+1}\sum_{n=0}^{\infty}\left(\frac{Ai(0)}{Ai'(0)}\right)^n\left(\frac{K}{\exp(\theta)+1}\right)^n\frac{\chi^{n/3}}{\Gamma\left(\frac{n+3}{3}\right)} \quad (66)$$

Considering the high K_{het} limit the following result is obtained:

$$\frac{L[A]}{[A]_{bulk}} = \frac{1}{s}\left(1 - \frac{Ai(s^{1/3}\xi)}{Ai(0)} - \frac{s^{1/3}\,Ai'(0)\,Ai(s^{1/3}\xi)}{K_{het}\,Ai(0)^2}\,\frac{1}{1-(\exp(\theta)+1)\frac{Ai'(0)}{Ai(0)}\frac{s^{1/3}}{K_{het}}}\right) \quad (67)$$

which gives a four-term approximation for the current−voltage behavior in this range:

$$\frac{I}{Fw\left(\frac{2v_o x_e^2 D^2}{h}\right)^{1/3}[A]_{bulk}} \approx \frac{-Ai'(0)}{Ai(0)}\left(\frac{1}{\Gamma(5/3)}\right) + \frac{\exp(\theta)}{\exp(\theta)+1}\sum_{n=1}^{4}\left(\frac{(\exp(\theta)+1)Ai'(0)}{Ai(0)K_{het}}\right)^n\frac{1}{\Gamma\left(\frac{5-n}{3}\right)} \quad (68)$$

Figure 8 shows voltammograms calculated for the heterogeneous EC mechanism for values of K_{het} in the range 0−8.0. For $K_{het} < 2.0$ eq 64 was used. The latter is slowly convergent; while for the case of $K_{het} = 1.0$, 20 terms were required to achieve convergence to within 1% over the entire range of θ values required, for $K_{het} = 2.0$, 1000 terms were needed. The voltammograms in Figure 8 with $K_{het} > 2.0$ were constructed, for convenience, using a mixture of eq 64 (for low currents) and eq 68 (for currents near the limiting value) as shown in Figure 8. The calculated voltammograms, such as those in Figure 8, permit the inference of the dependence of $\theta_{1/2}$ on K; this is

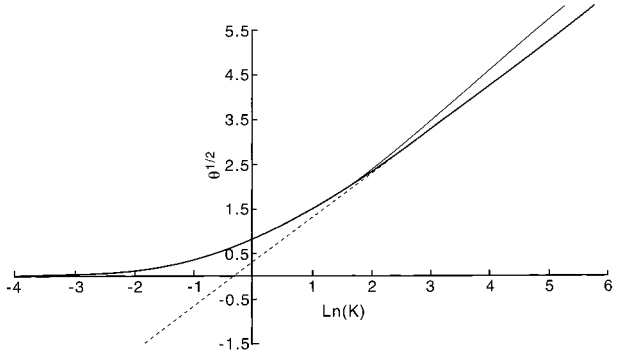

Figure 9. Variation of $\theta_{1/2}$ with ln K (bold line) as deduced from eq 64. In addition, the low K (eq 69) and high K (eq 70) approximations are shown.

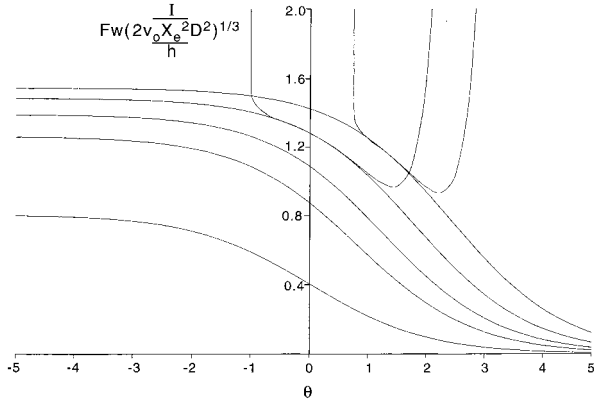

Figure 10. Current−voltage ($I-\theta$) curves calculated for the heterogeneous ECE mechanism, using eqs 73 and 74 for the following values of K: 0.0, 1.0, 2.0, 4.0, and 8.0.

shown in Figure 9. For $K < 5.0$ the curve shown can be described by the approximate equation

$$\theta_{1/2} = -0.0016(\ln K_{het})^4 + 0.0014(\ln K_{het})^3 + 0.1192(\ln K_{het})^2 + 0.5543(\ln K_{het}) + 0.8213 \quad (69)$$

to within 1%. For $K > 7.0$ the expression

$$\theta_{1/2} = 0.3131 + \ln K_{het} \quad (70)$$

was found to be valid. The result that the shift in half-wave potential in the high K limit is solely a function of K_{het} is implicit in eqs 64 and 68.

Last we turn to the heterogeneous ECE mechanism for which the current passed is evaluated using

$$I = Fw\int_0^{x_e} D\left(\frac{\partial[A]}{\partial y}\right)_{y=0} + k_{het}[B]_{y=0}\,dx \quad (71)$$

or

$$I = Fw\left(\frac{2v_o x_e^2 D^2}{h}\right)\int_0^1\left(\frac{\partial[A]}{\partial\xi}\right)_{\xi=0} + K_{het}[B]_{\xi=0}\,d\chi \quad (72)$$

Using the Nernst eq and eq 66 to find $[B]_{\xi=0}$, it can be established that the total current flowing is given, for low K_{het},

by

$$\frac{I}{Fw\left(\frac{2\upsilon_o x_e^2 D^2}{h}\right)^{1/3}[A]_{bulk}} = \frac{-Ai'(0)}{Ai(0)(\exp(\theta)+1)\Gamma(5/3)} + \frac{2\exp(\theta)+1}{\exp(\theta)+1}\sum_1^\infty \left(\frac{Ai(0)}{Ai'(0)}\right)^{n-1}\left(\frac{K_{het}}{(\exp(\theta)+1)}\right)^n \frac{1}{\Gamma\left(\frac{n+5}{3}\right)} \quad (73)$$

and at high K_{het} by the approximation

$$\frac{I}{Fw\left(\frac{2\upsilon_o x_e^2 D^2}{h}\right)^{1/3}[A]_{bulk}} \approx \frac{-Ai'(0)}{Ai(0)}\left(\frac{2}{\Gamma(5/3)}\right) + \frac{2\exp(\theta)+1}{\exp(\theta)+1}\sum_{n=1}^4 \left(\frac{(\exp(\theta)+1)Ai'(0)}{Ai(0)\,K_{het}}\right)^n \frac{1}{\Gamma\left(\frac{5-n}{3}\right)} \quad (74)$$

Alternatively, in terms of the effective number of electrons, N_{eff}, passed in the ECE process, we have at low K_{het}

$$\left[\sum_0^\infty \left(\frac{Ai(0)}{Ai'(0)}\right)^n \left(\frac{K_{het}}{(\exp(\theta)+1)}\right)^{n+1} \frac{1}{\Gamma\left(\frac{n+6}{3}\right)}\right] / \left[\frac{-Ai'(0)}{Ai(0)(\exp(\theta)+1)\Gamma(5/3)} + \frac{\exp(\theta)}{(\exp(\theta)+1)}\sum_0^\infty \left(\frac{Ai(0)}{Ai'(0)}\right)^n \left(\frac{K_{het}}{(\exp(\theta)+1)}\right)^{n+1} \frac{1}{\Gamma\left(\frac{n+6}{3}\right)}\right] = N_{eff} - 1 \quad (75)$$

while for high K_{het}

$$\left[\sum_{n=1}^4 \left(\frac{(\exp(\theta)+1)Ai'(0)}{Ai(0)\,K_{het}}\right)^n \frac{1}{\Gamma\left(\frac{5-n}{3}\right)}\right] / \left[\frac{\exp(\theta)+1}{\Gamma(5/3)} + \exp(\theta)\sum_1^4 \left(\frac{(\exp(\theta)+1)Ai'(0)}{Ai(0)\,K_{het}}\right)^n \frac{1}{\Gamma\left(\frac{5-n}{3}\right)}\right] = N_{eff} - 2 \quad (76)$$

Figure 10 shows voltammograms calculated using eqs 73 and 74 for K_{het} values in the range 0−8.0. The convergence behavior was as found for the heterogeneous EC case above. The voltammograms have exactly the same shape as for the latter case as expected for a reversible process (eq 44) except that they are multiplied by the factor of N_{eff} given in eqs 75 and 76 as appropriate.

Conclusions

Simple analytical results have been generated to describe the voltammetric wave shape and its dependence on the coupled kinetics for the cases of both homogeneous and heterogeneous EC and ECE processes.

References and Notes

(1) Cooper, J. A.; Compton, R. G. *Electroanalysis* **1998**, *10*, 141.

(2) Compton, R. G.; Pilkington, M. B. G.; Stearn, G. M. *J. Chem. Soc., Faraday Trans. 1* **1988**, *84*, 2155.

(3) Fisher, A. C.; Compton, R. G. *J. Phys. Chem.* **1991**, *95*, 7538.

(4) Alden, J. A.; Feldman, M. A.; Hill, E.; Prieto, F.; Oyama, M.; Coles, B. A.; Compton, R. G.; Dobson, P.; Leigh, P. A. *Anal. Chem.* **1998**, *70*, 1707.

(5) Aixill, W. J.; Alden, J. A.; Prieto, F.; Waller, G. A.; Compton, R. G.; Rueda, M. *J. Phys. Chem. B* **1998**, *102*, 1515.

(6) Compton, R. G.; Dryfe, R. A. W. *Prog. React. Kinet.* **1995**, *20*, 245.

(7) Cooper, J. A.; Alden, J. A.; Oyama, M.; Compton, R. G.; Okazaki, S. *J. Electroanal. Chem.* **1998**, *442*, 201.

(8) Compton, R. G.; Eklund, J. C.; Nei, L.; Mah, Y. A.; Colton, R.; Bond, A. M. *J. Electroanal. Chem.* **1995**, *385*, 249.

(9) Compton, R. G.; Pilkington, M. B. G. *J. Chem. Soc., Faraday Trans. 1* **1989**, *85*, 2255.

(10) Compton, R. G.; Alden, J. A.; Cooper, J. A.; Hutchison, F.; Prieto, F. *J. Electroanal. Chem.* **1997**, *432*, 63.

(11) Coles, B. A.; Compton, R. G.; Spackman, R. A. *Electroanalysis* **1993**, *5*, 41.

(12) Speiser, B. *Electroanal. Chem.* **1996**, *19*, 24.

(13) Compton, R. G.; Fisher, A. C.; Wellington, R. G.; Dobson, P. J.; Leigh, P. A. *J. Phys. Chem.* **1993**, *97*, 10410.

(14) Lévêque, M. A. *Ann. Mines. Mem. Ser.* **1928**, *12/13*, 201.

(15) Miles, J. *Integral Transforms in Applied Mathematics*; Cambridge University Press: Cambridge, U.K., 1965.

(16) Copson, E. T. *Asymptotic Expansions*; Cambridge University Press: Cambridge, U.K., 1965.

(17) Abramowitz, M.; Stegun, I. A. *Handbook of Mathematical Functions*; Dover: New York, 1970.

(18) Leslie, W. M.; Alden, J. A.; Compton, R. G.; Silk, T. *J. Phys. Chem.* **1996**, *100*, 14130.